Circulation responses to snow albedo feedback in climate change

Christopher G. Fletcher and Paul J. Kushner

Department of Physics, University of Toronto, 60 St George St, Toronto,

M5S 1A7, Canada.

Alex Hall and Xin Qu

Department of Atmospheric and Oceanic Sciences, University of California,

Los Angeles, United States.

C. G. Fletcher, Department of Physics, University of Toronto, 60 St George St, Toronto, M5S 1A7, Canada. (chris.fletcher@utoronto.ca)

Climate change is expected to cause a reduction in the spatial extent of snow cover on land. Recent work suggests that this will exert a local influence on the atmosphere and the hydrology of snow-margin areas through the snow-albedo feedback (SAF) mechanism. A significant fraction of variability among IPCC AR4 general circulation model (GCM) predictions for future summertime climate change over these areas is related to the models' representation of springtime SAF. In this study, we demonstrate a nonlocal influence of SAF on the summertime circulation in the extratropical Northern Hemisphere. Increased land surface warming in models with stronger SAF is associated with large-scale sea-level pressure anomalies over the northern oceans and a poleward intensified subtropical jet. We find that up to 20-30% of the intermodel spread in projections of the circulation response to climate change is linearly related to SAF strength.

1. Introduction

Recent work has shown that there is a threefold spread in the strength of the simulated snow albedo feedback (SAF) among the current generation of general circulation models used in the Fourth Assessment Report (AR4) of the Intergovernmental Panel on Climate Change [*IPCC, 2007; Qu and Hall, 2007*]. This spread is explained mostly by the spread in the albedo values of snow-covered surfaces among the different models [*Qu and Hall, 2007*], and limited observational data has made it difficult to obtain a realistic reference value. The range in the models' SAF strength is shown to have a direct impact on the spread in projections of climate change over the continental interior of North America [*Hall et al.*, 2008]. Models with stronger SAF predict that summers will become warmer and drier than summers in models with weaker SAF.

It is unclear whether this warming and drying over land associated with SAF could also produce a teleconnected response in the atmospheric circulation. Previous work focusing on the fall-winter season has shown that the large-scale atmospheric circulation responds significantly on seasonal timescales to changes in surface temperature associated with variations in surface albedo caused by continental snow cover anomalies [*Cohen and Entekhabi*, 1999; *Fletcher et al.*, 2008]. Here, we focus on the summer season to investigate whether the variation in SAF among climate models exerts a control over projections of the atmospheric circulation response to climate change.

To our knowledge, the effects on the atmospheric circulation response to anthropogenic forcing from a radiative feedback such as SAF have not been previously explored. In this letter, we demonstrate that SAF affects not only the spread of the surface temperature

responses to climate change, but also the spread of atmospheric circulation responses. This hemispheric-scale signal is most significant close to the surface, but is also found to project onto the zonal mean circulation in the form of a poleward intensification of the subtropical jet. We quantify the influence of SAF and find that up to 20-30% of the intermodel spread in projections of the circulation response to climate change is linearly related to SAF strength.

2. Data and Methods

All data are taken from the the World Climate Research Programme's (WCRP's) Coupled Model Intercomparison Project phase 3 (CMIP3) multi-model dataset. We use 17 of the 18 CMIP3 models examined in *Qu and Hall* [2007] (henceforth "the models"); the exception being the ECHO-G model, which did not provide data on pressure levels. We define the response to climate change as the difference between the time average fields for the 2100s minus the 1900s.

The period of analysis is the summer season, when *Hall et al.* [2008] found a strong influence of SAF on surface warming and the hydrological cycle; all figures are presented for the June-July-August (JJA) mean. We use an index of SAF for spring as described in *Qu and Hall* [2007], which is representative of SAF strength throughout the year. This index is regressed onto summertime fields of the response to climate change to form a regression pattern $\mathbf{Y}$, where

$$\mathbf{Y} = \mathbf{X} \cdot \mathbf{S}, \tag{1}$$

where $\mathbf{X}$ is the size M $\times$ N matrix of responses at M gridpoint locations for N models and $\mathbf{S}$ is the size N matrix of SAF values, which are standardized to have zero mean and unit

variance. **Y** therefore has the same units as **X**, and represents the response in **X** per unit standard deviation in the SAF index.

Each of the models assessed in this study predicts a warming response to climate change in JJA mean surface temperature over Northern Hemisphere (NH) land areas. However, the amplitude of the warming varies in the range 2.6 – 6.2 K with a mean of 4.4 K. Since the external radiative forcing is identical in all models, the spread in the temperature predictions must result from differences in the models' internal climate feedbacks, of which SAF is a likely contributor over extratropical land areas [*Qu and Hall*, 2007].

3. Results

3.1. Surface Response Associated with SAF

Figure 1a shows that models with stronger SAF produce a larger surface warming response to climate change. This is especially evident over the midlatitude regions of the NH continents, where local amplification of the greenhouse gas-induced warming is expected due to SAF [*IPCC, 2007*, Section 4.2.2.1]. In agreement with Fig. 2a of *Hall et al.* [2008] the strongest and most significant warming response is seen over North America, where recent negative trends in springtime snow cover are largest [*Groisman et al.*, 2004]. A similar, but weaker, signal is seen over Eurasia, which peaks over Northern India and the Tibetan Plateau.

Our principal result is that SAF is also associated with nonlocal circulation changes. This is suggested by an area of significant warming over the North Pacific (Fig. 1a), and clearly shown in the sea level pressure (SLP) response (Fig. 1b) with opposite-signed anomalies between the continents and northern oceans. This pattern represents a ther-

mally direct dynamical response associated with SAF: the land surface warms faster than the ocean, which drives surface divergence over the land and convergence over the ocean. The significant high pressure centers over the Azores and Aleutian regions indicate a poleward intensification of the quasi-permanent patterns that feed into the summer tropical trade winds. The concomitant 1000 hPa wind response (Fig. 1c) shows strengthened easterlies over the Pacific and Atlantic sectors around 40°N.

Over the Arctic basin the surface responses associated with SAF are very weak (Figs. 1a-c), which suggests that SAF does not exert a significant control over surface warming or circulation changes in that region. By contrast, the sea-ice albedo feedback has been shown to significantly amplify climate change over the Arctic in observations [*Deser et al.*, 2000] and models [*Holland and Bitz*, 2003]. The simulated SAF therefore appears to be acting independently of sea-ice albedo feedback in these models.

3.2. Response in the Free Troposphere

The influence of SAF on the circulation response to climate change is not confined to the surface. Figure 2 shows that SAF is associated with a vertically coherent response throughout much of the troposphere that projects significantly onto the zonal mean circulation. Stronger SAF is related to a broad region of mid-tropospheric warming centered on 50°N (Fig. 2a) and a dipolar zonal wind response that peaks in the upper troposphere and that appears to be in thermal wind balance with the warming (Fig. 2b). Consistently, the geopotential response corresponds to increased thickness throughout the troposphere in the 40°N-60°N region where SAF is strongest (Fig. 2c). Thus the SAF related forcing, which represents how GCMs simulate snow-related land surface processes, gives rise

to a deep zonal-mean response of the atmospheric general circulation. This zonal-mean response links stronger SAF with a poleward shifted subtropical jet (Fig. 2b) and with relatively enhanced dry static stability in the midlatitude lower troposphere (Fig. 2a). To our knowledge such a link has not been previously discussed and would probably not have been predicted a priori.

The earlier discussion was focused on the thermally direct dynamical response to climate change associated with SAF. Interestingly, the response also appears to have an indirect component. In particular, there is a weak but significant projection of the response onto the summertime planetary waves. Figure 3a shows that the quasi-stationary eddy geopotential height along 50°N is significantly perturbed over Eurasia, with the surface low at 90°E extending up to the tropopause. Furthermore, the surface high over the North Pacific (Fig. 1b) appears to form part of a downstream wave-train that is vertically coherent through the troposphere, indicating an equivalent barotropic structure.

Figure 3b demonstrates an asymmetry in this thermally indirect response between Eurasia and North America. Although North America shows the strongest warming associated with SAF (Fig. 1a), the surface low over North America and its associated downstream high (Fig. 1b) appear to be surface-trapped. Therefore, the response over North America is baroclinic, which is characteristic of a thermally direct dynamical response to the surface heating. By contrast, over Eurasia the circulation pattern is a barotropic wave-train, indicating a thermally indirect response. We discuss possible causes of this asymmetry in Section 4.

3.3. Reduction in the Spread of Projections

Following *Hall et al.* [2008] we next investigate whether any of the spread in the projections of the circulation response to climate change can be explained by the relationship between the circulation and SAF. *Hall et al.* found a one-third reduction in the inter-model standard deviation of projections of the surface temperature response over the United States after removing the component of the response that was linearly related to SAF.

In Fig. 4 we employ a similar diagnostic to grids of NH surface temperature, sea-level pressure and 1000 hPa winds. The largest reductions in the spread among the models are observed where the strongest and most significant responses were seen in Fig.1. In particular, the spread is reduced by 20-30% in (a) surface temperature over North America and Eurasia, (b) sea-level pressure over the Aleutian and Azores regions and (c) 1000 hPa wind over the North Pacific basin. This confirms that SAF exerts a significant control over the models' large-scale teleconnected circulation response to climate change, particularly over the North Pacific sector.

We have also performed a similar analysis (not shown) for temperature, geopotential height and wind fields at vertical levels in the middle and upper troposphere, as well as for the quasi-stationary wave field. A portion of the spread among the models in these fields is found to be linearly related to SAF, although the reduction in spread is generally weaker ($\sim$10-15%) than for the near-surface fields shown in Fig. 4.

4. Discussion and Conclusions

We have shown that projections of the summertime atmospheric circulation response to climate change among 17 CMIP3 models contain a significant component that is related to the strength of the simulated snow-albedo feedback (SAF). Models with stronger SAF are associated with both thermally direct and indirect circulation responses. The direct response involves increased warming over continental interiors, formation of collocated thermal low pressure centers and an intensification of the quasi-permanent summertime high pressure systems over the North Pacific and North Atlantic basins. This response projects onto the zonal mean circulation as a poleward intensified subtropical jet. The most significant signal is located in the Northern Hemisphere extratropics; SAF is not found to be a major contributor to circulation changes over the Arctic region.

The thermally indirect part of the response is dominant over the Eurasian sector and exhibits a barotropic projection onto the summertime quasi-stationary wave pattern. Over the North American sector the response is surface-trapped and weakly baroclinic. More realistic representation of SAF in models would help to constrain the intermodel spread in projections of the circulation response to anthropogenic forcing.

While the surface responses over North America and Eurasia are qualitatively similar, in the free troposphere the patterns are very different. This asymmetry raises the question: if the simplest dynamical model of the response associated with SAF is a thermally direct circulation, why does the response over Eurasia appear thermally indirect? One possible reason is that the planetary wave response to surface perturbations over Eurasia is enhanced by the presence of high topography [e.g., *Gong et al., 2004*], whereas over

North America the response is less sensitive to topographic barriers. Another is that the CMIP3 models project snow cover to increase (decrease) over eastern (western) Eurasia, while over North America the change is more zonally uniform (not shown). This could create a zonal asymmetry in the SAF-related surface forcing over Eurasia and, as a result, the thermally indirect response is dominant. This is the subject of ongoing analysis in experiments using full and idealized GCMs.

Finally, while the focus in this letter has been on the summertime dynamical response to climate change, we note that signals associated with SAF are also found during spring and fall, and in precipitation and soil moisture fields (results not shown). In particular, it appears that the response of the Indian Monsoon circulation is significantly related to the strength of SAF. However, the relationship between the Monsoon and SAF is complex [e.g., *Fasullo, 2004*] and distinct from the discussion in this letter; it will therefore be left to a future contribution.

Acknowledgments. We acknowledge the modeling groups, the Program for Climate Model Diagnosis and Intercomparison (PCMDI) and the WCRP's Working Group on Coupled Modeling (WGCM) for their roles in making available the WCRP CMIP3 multi-model dataset. Support of this dataset is provided by the Office of Science, U.S. Department of Energy. C.G.F and P.J.K acknowledge support from the Canadian Cryosphere Network and Canadian Foundation for Climate and Atmospheric Science.

References

Cohen, J., and D. Entekhabi, Eurasian snow cover variability and Northern Hemisphere climate predictability, *Geophys. Res. Lett.*, *26*(3), 345–348, 1999.

Deser, C., J. Walsh, and M. Timlin, Arctic sea ice variability in the context of recent atmospheric circulation trends, *J. Climate*, *13*(3), 617–633, 2000.

Fasullo, J., A stratified diagnosis of the Indian monsoon-Eurasian snow cover relationship, *17*(5), 1110–1122, 2004.

Fletcher, C. G., S. C. Hardiman, P. J. Kushner, and J. Cohen, The dynamical response to snow cover perturbations in a large ensemble of atmospheric GCM integrations, *J. Climate*, in press, 2008.

Gong, G., D. Entekhabi, and J. Cohen, Relative impacts of Siberian and north American snow anomalies on the winter Arctic Oscillation, *Geophys. Res. Lett.*, *30*(16), doi:10.1029/2003GL017749, 2003.

Gong, G., D. Entekhabi, and J. Cohen, Orographic Constraints on a Modeled Siberian Snow-Tropospheric-Stratospheric Teleconnection Pathway, *J. Climate*, *17*, 1176–1189, 2004.

Groisman, P., R. Knight, T. Karl, D. Easterling, B. Sun, and J. Lawrimore, Contemporary changes of the hydrological cycle over the contiguous United States: Trends derived from in situ observations, *J. Hydromet*, *5*(1), 64–85, 2004.

Hall, A., X. Qu, and J. D. Neelin, Improving predictions of summer climate change in the United States, *Geophys. Res. Lett.*, *35*(1), doi:10.1029/2007GL032012, 2008.

196 Holland, M., and C. Bitz, Polar amplification of climate change in coupled models, *Climate*
197 *Dyn.*, *21*(3-4), 221–232, doi:10.1007/s00382-003-0332-6, 2003.
198 Qu, X., and A. Hall, What controls the strength of snow-albedo feedback?, *J. Climate*,
199 *20*(15), 3971–3981, doi:10.1175/JCLI4186.1, 2007.
200 IPCC, 2007: Solomon, S., D. Qin, M. Manning, Z. Chen, M. Marquis, K. Averyt, M. Tig-
201 nor, and H. Miller (Eds.), *Climate Change 2007: The Physical Science Basis. Contri-*
202 *bution of Working Group I to the Fourth Assessment Report of the Intergovernmental*
203 *Panel on Climate Change*, 996 pp., Cambridge University Press, Cambridge, United
204 Kingdom and New York, NY, USA, 2007.

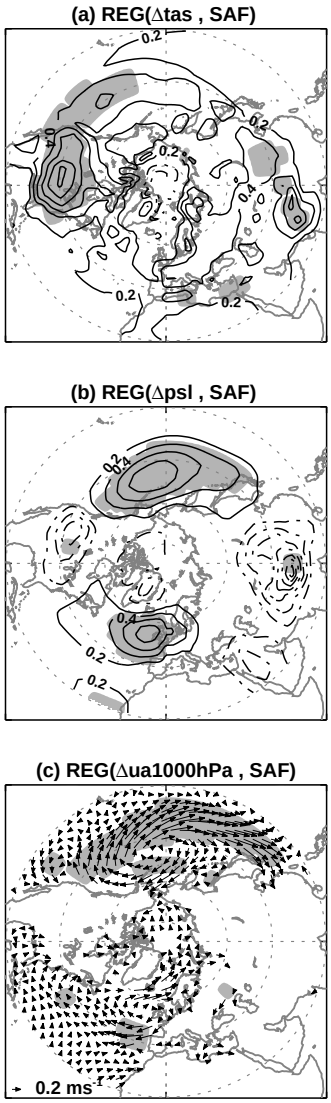

Figure 1. (a) Regression of the response to climate change (defined as the difference between the time means for the 22nd Century and the 20th Century) in surface temperature (Δtas) on the snow albedo feedback (SAF) index. The SAF index is calculated as the ratio of the response to climate change in surface albedo over the response to climate change in surface temperature in spring (March-April-May) over land areas poleward of 30°N. (b) as (a) except for mean sea level pressure (Δpsl) and (c) as (a) except for 1000 hPa wind vectors (Δua1000). Contour interval is (a) 0.2 K and (b) 0.2 hPa and negative contours are dashed. Reference wind vector is shown in bottom left of (c). Shading denotes responses that are statistically significant ($p < 0.05$) as determined by a Student's

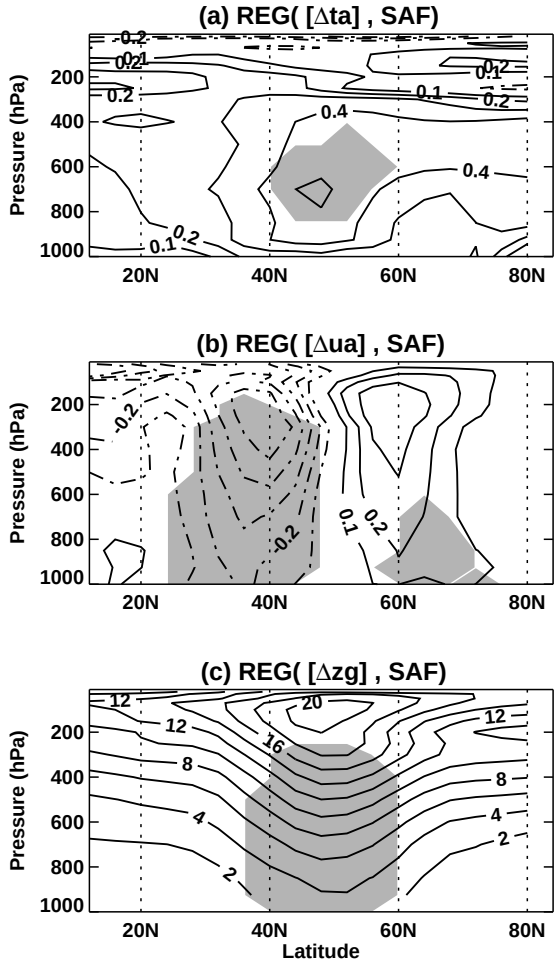

Figure 2. As Fig. 1a except fields plotted are (a) zonal mean temperature ([Δta]), (b) zonal mean zonal wind ([Δua]) and (c) zonal mean geopotential height ([Δzg]). Contour interval is (a) 0.1 K, (b) 0.1 m s^{-1} and (c) 2 m and negative contours are dashed. Shading as in Fig. 1a.

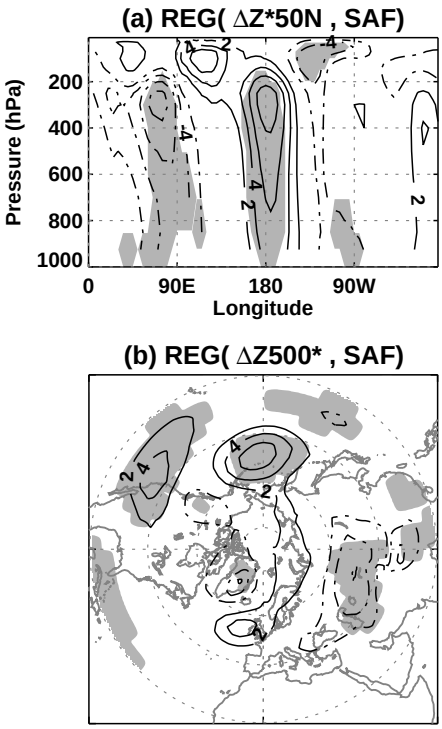

Figure 3. As Fig. 1a except fields plotted are (a) eddy geopotential height along 50°N (ΔZ^*50N) and (b) eddy geopotential height at 500 hPa ($\Delta Z500^*$). Contour interval is 2 m. Negative contours are dashed and shading as in Fig. 1a.

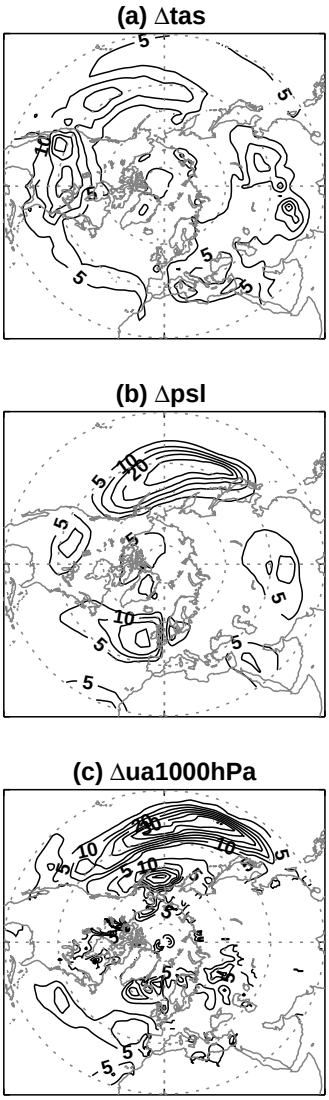

Figure 4. The percentage reduction in the inter-model standard deviation of responses to climate change after the component linearly related to SAF is removed. At each grid cell we perform a linear least-squares fit between SAF and the response variable. Plots show $(\sigma_{SAF\_REMOVED}/\sigma_{TOTAL}) \times 100\%$ for (a) surface temperature, (b) sea-level pressure and (c) 1000 hPa winds. Contour interval is 5%.